Leveraging Artificial Intelligence and Machine-Learning Methods for Bias Correction of Reference Evapotranspiration Utilizing ERA5 Data

Shadman Veysi[1]; Soheila Zarei, Ph.D.[2]; Eslam Galehban[3]; and Amir Tahooni[4]

Abstract: This study addresses the challenge of mitigating biases in daily reference evapotranspiration (ET_o) computations, utilizing the ECMWF Reanalysis version 5 reanalysis data set within coastal regions. Data from 14 weather stations across the coastal Caspian Sea basin covering the period of 2003–2023 were gathered to compute ET_o as a benchmark for bias correction. Therefore, five distinct artificial intelligence models, namely, artificial neural networks, gene expression programming, adaptive network-based fuzzy inference systems, random forest (RF), and support vector machine (SVM), were used to mitigate bias in daily ET_o. The results demonstrated that the RF model performed exceptionally well, achieving normalized root mean square error values below 10% and residual mean bias error values below 15%. It ranked as the top-performing model in eight out of the 14 stations during the testing phase. However, in the testing step, SVM has surpassed other methods in other stations. To provide a better perspective on the results, a map showcasing the top-performing methods based on minimizing bias for each station was presented. This research highlights the effectiveness of machine-learning methods for improving ET_o estimates. It demonstrates the potential for successful implementation of the RF method to bias correction of the Food and Agriculture Organization (FAO)–Penman–Montith equation fed by ERA5 climate data in basin scale. **DOI: 10.1061/JIDEDH.IRENG-10487.** *© 2025 American Society of Civil Engineers.*

Author keywords: Scarce data; Gridded data set; Long-term; Machine learning; Modification.

Introduction

Reference evapotranspiration (ET_o) is a crucial parameter in determining crop water requirement, directly impacting irrigation planning and agricultural water management (Allen et al. 1998). Accurate estimation of ET_o is essential for optimizing agricultural water management, particularly in irrigation scheduling and assessing crop water requirements (Pereira et al. 2021; Farooque et al. 2022; Granata and Di Nunno 2021). In addition, ET_o offers critical insights into regional climate behavior, aiding in broader water resource planning and climate impact assessments (Pereira et al. 2015). Despite its significance, inaccuracies in ET_o estimates, stemming from factors such as data quality and the availability of data, pose challenges for water management practices (Rahimikhoob et al. 2020; Sharma et al. 2022).

The era of starting computation of ET_o was based on the water budgets account method, which involves the utilization of grass lysimetric instruments to furnish precise and dependable measurements of water fluxes in control volume (López-Urrea et al. 2006). Despite the efficacy of this method, acquiring long-term lysimetric data presents considerable challenges (Barideh et al. 2022). Also, the result of this method extends in field scale decision-makers and develops to the large scale, which comes with uncertainty (Moyers et al. 2023).

Alternatively, climatic data from meteorological stations are often used with equations such as the FAO–Penman–Monteith model, which integrates diverse meteorological variables to estimate ET_o (Allen et al. 1998). This comprehensive equation integrates diverse climatic parameters, including solar radiation, wind speed, air temperature, and relative humidity. However, the availability of meteorological data is not guaranteed, and dealing with long-term and missing data poses another challenge for these methods (Almorox et al. 2015; Sentelhas et al. 2010). Also, the point measurements in land cover with biodiversity often introduce uncertainty. For example, the use of meteorological data from airport stations and within urban areas may introduce bias when estimating crop water requirement in agricultural lands (Veysi et al. 2024). However, the problem of extending results to a large scale comes with uncertainty.

Recently, the field of remote sensing, specifically the branch of reanalysis data sets, has emerged, offering historical global climatic data with different hourly and daily times and different spatial resolutions (i.e., 80, 31, and 11 km) without missing data on a global scale (Hersbach et al. 2020; Veysi et al. 2023b; Pelosi 2023; Veysi and Galehban 2024). One of the famous data sets in this area is ERA5, which was developed by the European Centre for Medium-Range Weather Forecasts (ECMWF). Although reanalysis data sets are widely used, they face significant challenges in accuracy, with biases reported to range between 15% and 30% at daily time scales. Previous studies have highlighted the limitations of reanalysis data sets such as ERA5 in capturing localized climatic variations, particularly in regions with complex topographies. Addressing these biases is critical for improving the applicability of ET_o estimates in water management frameworks. (Martins et al. 2017; Raziei and Parehkar 2021). This level of bias is particularly critical for determining the ET_o values specifically when the target is to estimate crop water

[1]Assistant Professor, Dept. of Irrigation and Soil Physics, Soil and Water Research Institute, Alborz 31785-311, Iran (corresponding author). Email: sh.veysi@areeo.ac.ir

[2]Dept. of Irrigation and Reclamation Engineering, Univ. of Tehran, Tehran 31587-77871, Iran. Email: soheila_zareie@yahoo.com

[3]Ph.D. Student, Dept. of Remote Sensing and GIS, Univ. of Tehran, Tehran 4665-14155, Iran. Email: galehban_eslam@yahoo.com

[4]Ph.D. Student, Dept. of Remote Sensing and GIS, Univ. of Tehran, Tehran 4665-14155, Iran. Email: amir.tahooni@ut.ac.ir

Note. This manuscript was submitted on September 9, 2024; approved on March 6, 2025; published online on May 29, 2025. Discussion period open until October 29, 2025; separate discussions must be submitted for individual papers. This paper is part of the ***Journal of Irrigation and Drainage Engineering***, © ASCE, ISSN 0733-9437.

requirements of crops such as rice, which is the most water-intensive crop in Iran, posing challenges in the northern regions. Therefore, before using these data at the first stage, bias correction is needed.

The commonly employed correction techniques mainly involve mean-based scaling and transformations based on probability distribution mapping (Chen et al. 2013; Ji et al. 2020). Mean-based scaling is a straightforward bias correction method that adjusts the mean of ET_o from reanalysis data (ERA5) and the mean of observed data, assuming that the bias remains constant over time (Paredes et al. 2017). However, this method is not suitable for variables such as ET_o, which exhibit significant spatial and temporal variability. Another common method used for bias correction of ET_o data is the generalized linear model (GLM) (Srivastava et al. 2015). GLMs calibrate each parameter linearly, which can be problematic because the relationships between the factors influencing ET_o (such as latitude, longitude, and altitude) are often nonlinear. This can result in an exclusive linear regression for each station and climate zone (Elagib et al. 2024).

Recently researchers have explored the application of artificial intelligence methods to predict ET_o (Landeras et al. 2008; Yassin et al. 2016; Traore et al. 2016; Shiri 2017; Gong et al. 2016; Keshtegar et al. 2018; Tao et al. 2018) and, also, machine-learning techniques (Mohammadrezapour et al. 2019). These methods have demonstrated their capability for precise predictions for hydrological variables, including ET_o, and are highly effective in handling complex, nonlinear relationships within data. They are flexible in handling complex data and are able to generalize to new situations, making them valuable tools for researchers in forecasting nonlinear events. While previous studies have employed reanalysis ET_o comparing with ET_o obtained from field data, this research focuses on a bias correction framework for reanalysis ET_o to improve the accuracy using artificial intelligence/machine learning (AI/ML) in a coastal region with a different climate.

The coastal zone along the Caspian Sea in northern Iran is known for its extensive paddy rice cultivation, which thrives under near-soil saturation and submersion conditions (Nasrabadi et al. 2011). The water needs of the rice closely match the ET_o, making bias correction of ET_o from reanalysis data sets critical to reduce statistical bias to less than 10% on a daily scale. Different stations were chosen along the Caspian Sea to cover diverse climates and select the best model for each area. However, the region has only 14 National Meteorological Stations, about one per 670 km^2, which is inadequate for its complex climate. Thus, thorough applicability assessments using reanalysis data sets are essential. The objectives of the present study were (1) to see how accurate the ET_o computed using reanalysis products is compared to FPM-ET_o calculated from observations; (2) to improve the accuracy of ET_o calculated using reanalysis by correcting biases found with observations ET_o and assess the resulting accuracy; and (3) to evaluate the top-performing AI/ML bias correction methods enhancing the approach's suitability for data-scarce regions.

Material and Methods

Study Area

The Caspian Sea, situated in northern Iran, encompasses the provinces of Gilan, Mazandaran, and Golestan. This region is often referred to as Iran's *rice bowl* due to its vital agricultural significance. Despite this, the region lacks sufficient synoptic stations, with only 14 of the 28 coastal cities having such stations, which could impact agricultural practices (Fig. 1). This study used ground-based weather data from these 14 stations, covering the years of 2003 to 2023.

Subsequently, Table 1 provides an overview of the averaged statistical information. The table includes T_{max} and T_{min} (daily maximum and minimum air temperature). Additionally, it encompasses RS (incoming shortwave solar radiation) presented in $W \cdot m^{-2}$ and wind speed at 2 m expressed in $m \cdot s^{-1}$.

Data Source

In-Suite ETo

Daily meteorological data from 14 synoptic stations, covering a 21-year period (2003–2023), were sourced from the Iran Meteorological Organization (IRIMO) and meteorological quality-controlled by the IRIMO. The in-suite used T_{min}, T_{max}, U_2, SR, and RH. ET_o was calculated using the FAO–Penman–Monteith equation implemented through the REF-ET software, as described in Eq. (1). The Penman–Monteith equation is the global standard for estimating ET_o because it integrates energy balance and aerodynamic factors, providing robust and adaptable results across various climates. Endorsed by FAO, it ensures consistency and

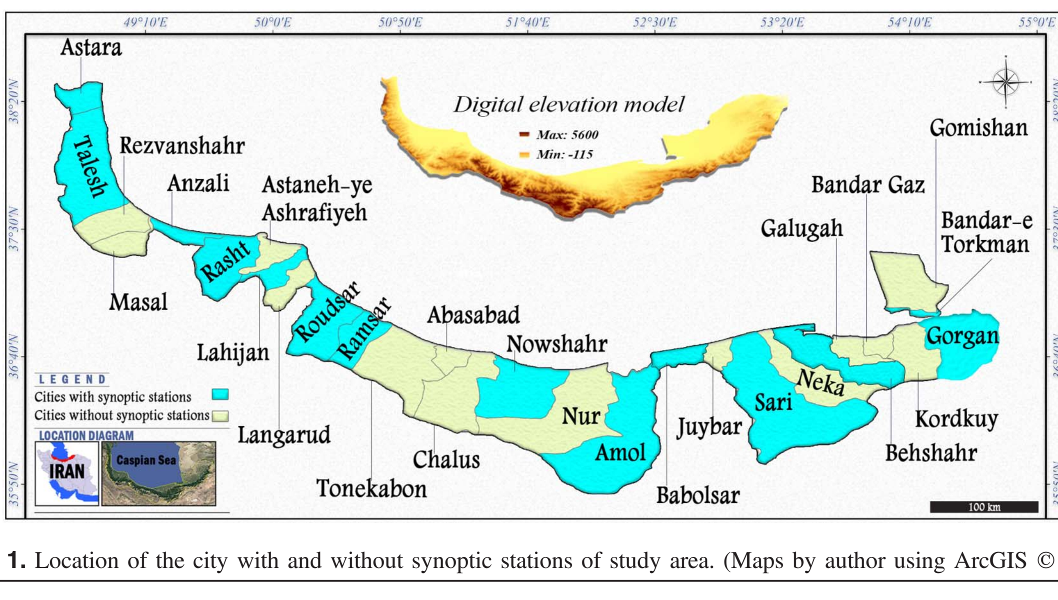

Fig. 1. Location of the city with and without synoptic stations of study area. (Maps by author using ArcGIS © Esri.)

Table 1. Main statistics of the selected weather stations in coastline of Caspian Sea sites

No.	Name	Elevation (m)	Longitude (°E)	Latitude (°N)	T_{min} (°C)	T_{max} (°C)	Rs (W/m^2)	Wind (m/s)
1	Amol	80	52.38	36.47	13.6	22.08	13.83	1.93
2	Anzali	−26	49.46	37.48	14.78	19.83	14.64	2.48
3	Astara	−24	48.85	38.37	12.33	19.72	14.14	1.2
4	Babolsar	−25	52.64	36.70	14.62	21.71	14.91	1.75
5	Bandar-e Torkman	−26	54.07	36.90	14.27	22.36	15.32	3.50
6	Lahijan	−4	50.02	37.19	12.12	21.28	13.89	1.48
7	Nowshahr	−14	51.47	36.66	13.38	20.30	14.07	1.96
8	Ramsar	−14	50.68	36.90	13.95	20.18	13.28	1.86
9	Rasht	19	49.65	37.20	12.18	21.40	13.74	1.70
10	Roudsar	−22	50.32	37.12	12.85	20.32	13.54	1.88
11	Sari	30	52.99	36.54	13.59	22.63	14.20	1.13
12	Talesh	4	48.90	37.84	12.83	19.86	12.63	1.79
13	Behshahr	−15	53.38	36.85	14.19	21.37	15.28	2.81
14	Gorgan	−15	54.41	36.91	12.84	23.84	15.37	2.01

reliability in agricultural water management. However, the accuracy of ET_o estimates depends on precise input data, including radiation, wind speed, temperature, and humidity. Errors in these parameters can lead to significant deviations, highlighting the need for high-quality, site-specific measurements for optimal application

$$ET_o = \frac{0.408\Delta(R_n - G) + \gamma\frac{900}{T+273}u_2(e_s - e_a)}{\Delta + \gamma(1 + 0.34u_2)} \quad (1)$$

in which ET_o is in mm · day^{-1}; Δ = slope of the vapor pressure curve with respect to temperature (Kpa · °C^{-1}); R_n = net radiation (MJ · m^{-2} · d^{-1}); G = soil heat flux density (MJ · m^{-2} · d^{-1}); γ = psychometric constant (Kpa°C^{-1}); T = mean daily temperature (°C); e_s = saturation vapor pressure (mbar); e_a = actual vapor pressure of the air (mbar); and U_2 = wind speed at a height of 2 me above the ground (m · s^{-1}).

ET_o Using ERA5 Data Set

ERA5 reanalysis data, produced by the ECMWF, form a critical component of the Copernicus Climate Change Service in Europe. These open-access weather and climate data have a spatial resolution of 0.25° × 0.25°, making them an excellent resource for analyzing climate patterns and trends (Gebrechorkos et al. 2018). The spatial resolution of the ERA5 data is 31 km. To estimate ET_o in the coastline station, we obtained daily ERA5 data from 2003 to 2023 using the Google Earth Engine system in the city with the synoptic station Table 2.

Land Cover

The European Space Agency's (ESA's) land cover data are utilized to extract land cover fractions corresponding to cropland pixels in the Caspian Sea basin from coastlines of Caspian Sea basin. The land cover information for the year 2020, obtained at a resolution of 10 m, is depicted in Fig. 2. The ESA land cover product includes 12 classification schemes, derived from supervised classifications of Sentinel 1 and Sentinel 2 spectral data.

Climate Zone

This study utilized the reanalyzed Köppen–Geiger climate map (Rubel et al. 2017) to obtain climate data for 14 meteorological stations. The Köppen–Geiger climate data offer worldwide coverage with more details achieved through the use of downscaling algorithms to improve resolution to 5 arcmin. For additional details about the reanalyzed Köppen-Geiger climate map data, refer to the official source at Peel et al. (2007). The climate zone data extracted for the Caspian Sea coastline is illustrated in Fig. 3. The majority of stations (nine stations) are classified in temperature as *dry summer* or *hot summer*.

Artificial Intelligence and Machine Learning Methods

Three AI methods and two ML algorithms were employed for bias correction of ET_o using ERA5 reanalysis data sets, as these are among the most widely used techniques in the literature (Goyal et al. 2023) for daily ET_o estimation. Before applying each machine learning algorithm to model ET_o, it is crucial to optimize their hyperparameters (Mandal and Chanda 2023). Hyperparameter optimization prevents overfitting, ensuring reproducibility. Techniques such as grid search and random search systematically fine-tune algorithm parameters, enhancing performance and generalizability. This ensures that the machine learning models used for ET_o estimation are both reliable and efficient. Table 3 provides a detailed account of the specific hyperparameters adjusted for each machine learning algorithm.

Table 2. ERA5 data used for estimate reference evapotranspiration

Data	Abbreviate	Source	Spatial resolution	Temporal resolution	Range
Maximum temperature	T_{max}	ERA5	0.25° × 0.25°	Daily	2003–2023
Minimum temperature	T_{min}	ERA5	0.25° × 0.25°	Daily	
Average temperature	T_{mean}	ERA5	0.25° × 0.25°	Daily	
Dew point temperature	T_{dew}	ERA5	0.25° × 0.25°	Daily	
Wind speed	U_2	ERA5	0.25° × 0.25°	Daily	
Solar radiation	SR	ERA5	0.25° × 0.25°	Daily	

J. Irrig. Drain Eng., 2025, 151(4): 04025021

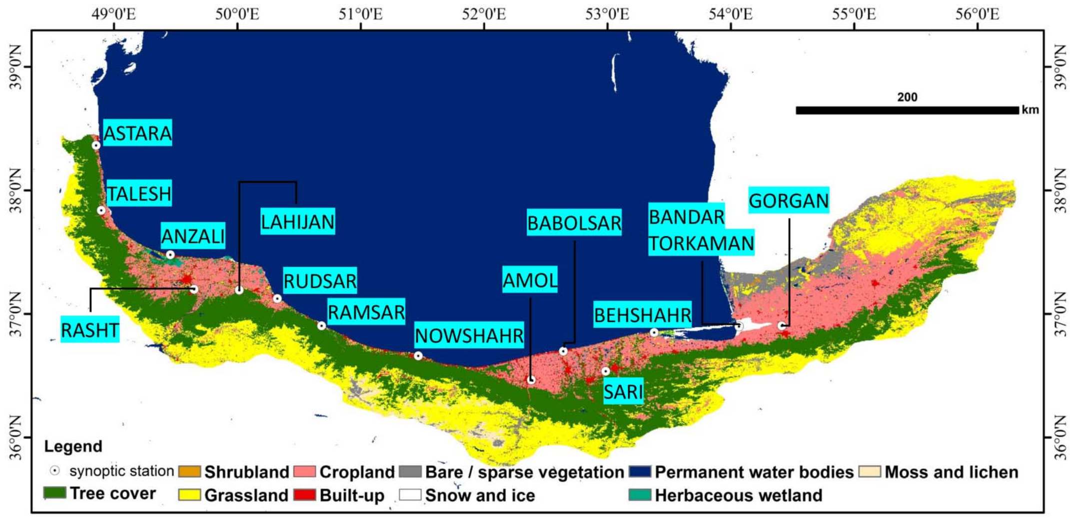

Fig. 2. Land cover data for the Caspian Sea coastline in 2020s.

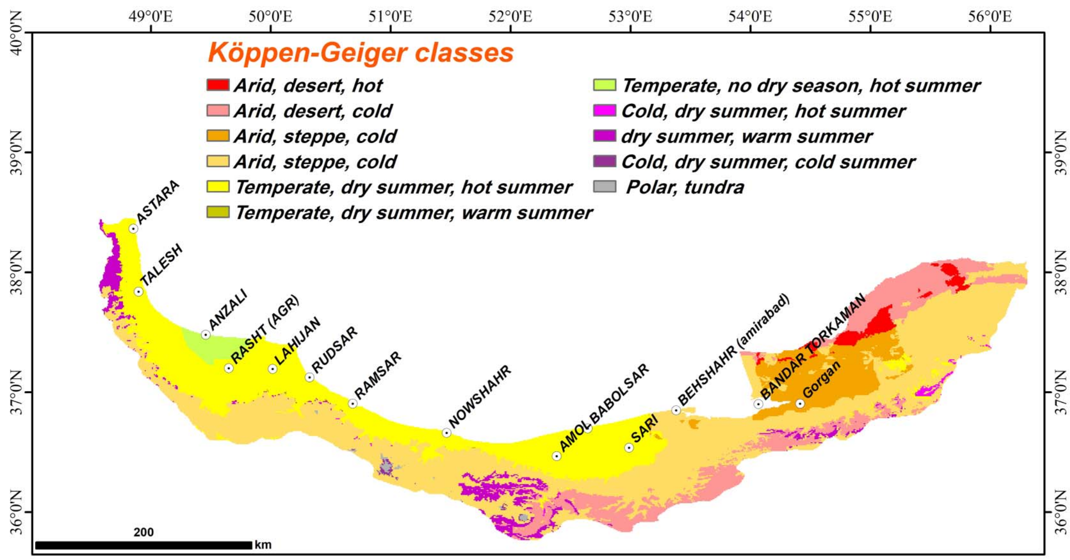

Fig. 3. Köppen–Geiger climate data extracted from the global reanalyzed.

Table 3. Configuration of hyperparameters tuned for each algorithm

Algorithm	Library used	Hyperparameters tuned	Hyperparameters tuned
SVM	Scikit-learn	gamma	[0.01, 0.05, 0.1, 0.2]
RF	Scikit-learn	n_estimators	[10, 20, 50, 100, 500, 1000]

Artificial Neural Network

Neural networks are widely used for processing nonlinear signals and typically consist of two or more layers of interconnected neurons (Nourani et al. 2020; Zakeri and Shankar 2022). The input layer takes in data, which are subsequently processed through one or more intermediate layers (Dimitriadou and Nikolakopoulos 2022). Finally, the output layer presents the network's results. During the learning process, the interconnection weights and neural biases are adjusted iteratively to minimize errors and enhance the network's performance (Ahmadaali et al. 2013; ZamanZad-Ghavidel et al. 2021). For this study, three-layer feed-forward neural networks were used with ERA5 climate data (T_{max}, T_{mean}, T_{min}, T_{dew}, SR, and $U2$) as input in Fig. 4. A sigmoid function was used in the hidden layer, and a linear function was used in the output layer. The number of hidden neurons was determined by trial and error. The learning algorithm adjusted weights and biases to enhance prediction accuracy and improve the network's generalization from the training data.

Gene Expression Programming

Genetic expression Programming (GEP) uses populations, fitness-based selection, and genetic operators to evolve solutions, similar

J. Irrig. Drain Eng., 2025, 151(4): 04025021

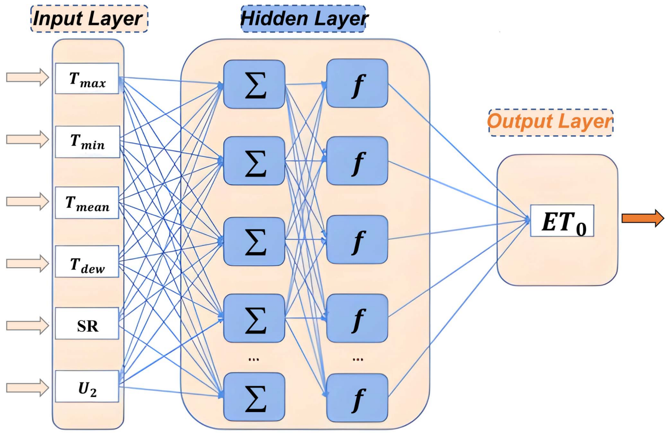

Fig. 4. Optimal neural network architecture for evapotranspiration modeling (ET_o).

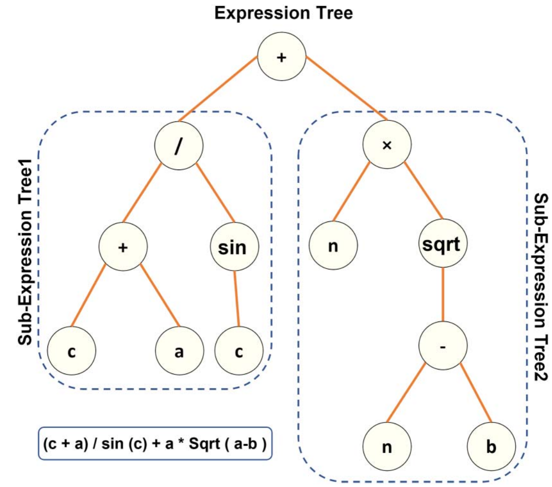

Fig. 5. Schematic of gene expression programming (GEP).

Table 4. Value of operators and parameters

No	Category	Parameter/operator	Value
1	Chromosomal structure	Number of chromosomes	30
		Head size	8
		Number of genes	3
		Linking function	Addition
2	Genetic operators	Mutation rate	0.044
		One-point recombination rate	0.3
		Two-point recombination rate	0.3
		Inversion rate	0.1
		Gene recombination rate	0.1
		IS transposition rate	0.1
		RIS transposition rate	0.1
		Gene transposition rate	0.1

Note: IS = insertion sequence transposition; and RIS = root insertion sequence transposition.

to genetic algorithms and genetic programming (Mehdizadeh and Kozekalani Sales 2018; Ferreira 2006). The method is data-driven and improves fitting based on adaptability to achieve the best solution using one or more genetic operators (Ferreira 2001; Mehr 2018). In this research, the GEP method is developed using the GeneXpro tool. Initially, GEP forms expression trees (chromosomes) for solving a specific problem (the first column in Table 4). Each expression tree comprises one or more genes known as sub-expression trees (sub-ET) Fig. 5. Each gene corresponds to a computer program that, when executed on data, produces the desired result. In the second stage of GEP, the fitness function is selected, with root mean square error (RMSE) chosen in this case (Shiri 2019). In the third stage, genetic operators are determined. Finally, a set of operators and functions is selected. This research employs various combinations of operators and functions, including +, −, *, /, sqrt(x), exp(x), Ln, $x\hat{2}$, $x\hat{3}$, $x(\hat{1}/3)$, sin(x), cos(x), and arctan(x).

Adaptive-Network-Based Fuzzy Inference Systems

Adaptive-network-based fuzzy inference systems (ANFIS) is a combination of neural network models and fuzzy logic (Jang 1993) used for modeling complex and nonlinear relationships. The objective of this amalgamation is to diminish computational time, specifically the duration required for convergence, while concurrently minimizing the error rate (Kisi and Zounemat-Kermani 2014). As illustrated in Fig. 6, the ANFIS structure consists of five layers (Karaboga and Kaya 2019). The first layer (the fuzzification

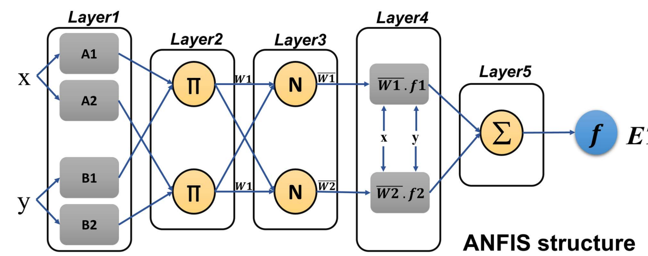

Fig. 6. Schematic of the adaptive-network-based fuzzy inference systems (ANFIS).

layer) employs various membership functions to extract membership values (μ_{A_i}, μ_{B_i}). The type of membership functions is determined through trial and error. In the second layer, fuzzy rules are considered in the form of Takagi and Sugeno (1985). If a fuzzy inference system with two input variables x and y and one output variable f is considered, a first-order Sugeno fuzzy model, which includes two IF-THEN fuzzy rules, is defined as follows:

$$f_1 = p_1A_1 +_1 B_1 + r_1 \tag{2}$$

$$f_2 = p_2A_2 + q_2B_2 + r_2 \tag{3}$$

In this model, f represents the output variable derived from a weighted average. The third layer, or normalization layer, calculates the normalized weight of each rule using fixed nodes. The fourth layer, or defuzzification layer, multiplies these normalized weights by the rule outputs (fi) to get weighted values [Eqs. (1) and (2)]. The fifth layer, or output layer, produces the final ETo value as the ANFIS result. ANFIS training combines error backpropagation with the least squares error method.

Random Forest

Random forest (RF) regression is an advanced ensemble machine learning technique that uses bootstrap resampling to create multiple random decision trees (Breiman 2001). Each tree is trained on a randomly selected subset of the training data Liaw (2002). Known for its strong predictive accuracy and ability to handle nonlinear, complex problems while preventing overfitting, RF is a highly effective method (Azadbakht et al. 2018; Belgiu and Drăguţ 2016).

J. Irrig. Drain Eng., 2025, 151(4): 04025021

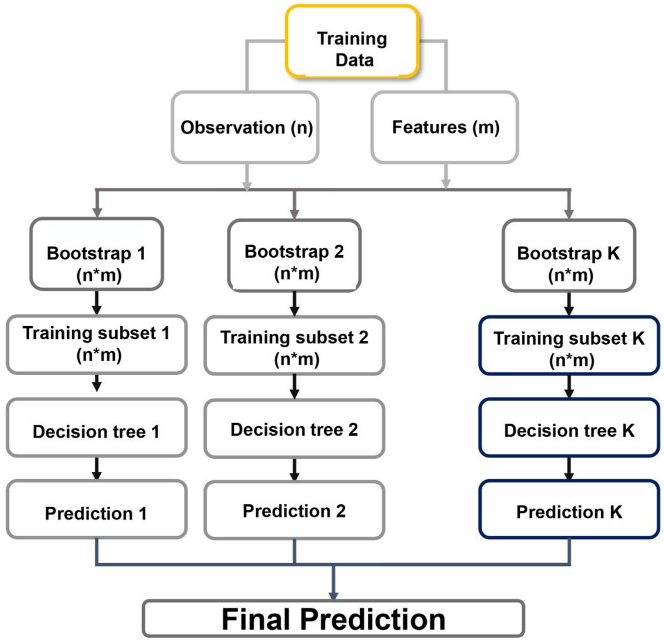

Fig. 7. Schematic of the random forest (RF).

RF is a representative bagging integrated learning algorithm. At its core, RF regression combines a multitude of decision trees and selects a subset of explanatory variables for each tree. Subsequently, individual decision tree yields specific predictions, with the algorithm then aggregating these predictions to derive the final regression outcome through averaging (Ebrahimy et al. 2021; Zhao et al. 2022). Fig. 7 shows a schematic of RF method steps for bias correction of ET_o.

Support Vector Machine

ET_o estimation was performed using a support vector machine (SVM) with a radial basis function (RBF) kernel, chosen for its superior performance over multiple linear regression and multiple nonlinear regression models (Khan and Coulibaly 2006; Yin et al. 2017). The RBF kernel is effective for ET_o prediction tasks. A grid search was used to select key support vectors and exclude nonsupport ones, reducing noise and improving efficiency (Deka 2014). To optimize the division of training, validation, and test sets, the *K*-cross-validation technique was applied (Eslamian et al. 2008; Fan et al. 2018; Wen et al. 2015).

ET_o *Bias Correction Framework*

This study introduces an ET_o bias correction framework with three key components: data collection, model development, and model selection. The ERA5 data set and station observations are used to reduce discrepancies between ET_o values from ERA5 and weather station measurements. The preprocessing stage clustered station data into two groups to calculate independent ET_o values, which were subsequently compared with the ERA5 reanalysis data. The model development phase includes building, calibrating, and validating models using AI techniques [artificial neural network (ANN), ANFIS, GEP] and machine learning methods (RF, SVM) to identify the best model. The choice of these models was guided by their proven effectiveness in handling complex, nonlinear relationships and their frequent use in hydrological modeling. ERA5 data serves as input, and daily ET_o from 14 stations provides the benchmark. The data set was split, with 70% for model construction and 30% for evaluation. The analysis was conducted using *R* software for coding the machine learning models and artificial intelligence techniques. Fig. 8 shows the conceptual framework and research steps.

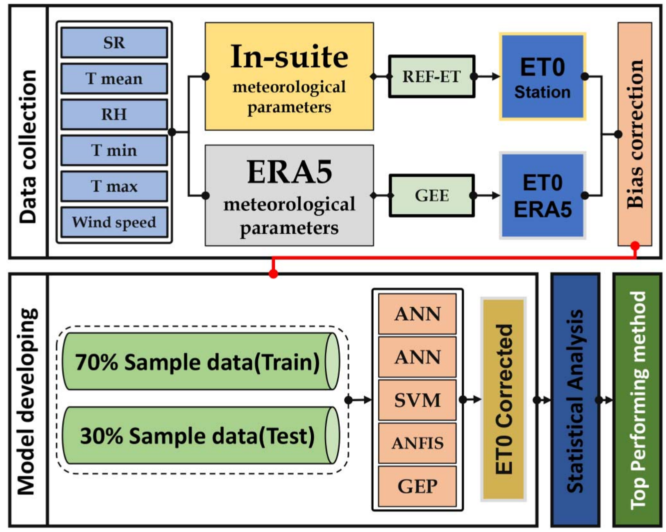

Fig. 8. Procedure of the ET_o bias correction framework.

Evaluation Metrics

Model predictions were evaluated against the FAO-56 ET_o derived from station observations. The accuracy of the simulated ET_o was assessed using four statistical error metrics, specifically the normalized root mean squared error (nRMSE) and residual mean bias error (rMBE), by comparing them to the observational ET_o data. These metrics are particularly suitable for this study because nRMSE quantifies the overall prediction accuracy by expressing the error as a percentage of the observed mean, making it easy to interpret and compare across data sets. Meanwhile, rMBE measures the bias in model predictions, indicating whether the model consistently overestimates or underestimates ET_o. Together, these metrics provide a comprehensive assessment of both accuracy and systematic bias, essential for validating model reliability

$$R^2 = \frac{(\sum_{i=1}^{n}(O_i - \bar{O})(P_i - \bar{P}))\hat{2}}{\sum_{i=1}^{n}(O_i - \bar{O})^2 \sum_{i=1}^{n}(P_i - \bar{P})^2} \tag{4}$$

$$\mathrm{RMSE} = \sqrt{\frac{1}{n}\sum_{i=1}^{n}(P_i - O_i)^2} \tag{5}$$

$$\mathrm{nRMSE} = \frac{\sqrt{\frac{1}{n}\sum_{i=1}^{n}(P_i - O_i)^2}}{\bar{O}} \tag{6}$$

$$\mathrm{rMBE} = \left(\frac{100}{\bar{O}}\right) \times \frac{1}{n}\sum_{i=1}^{n}(P_i - O_i)^2 \tag{7}$$

where O_i = observed ET_o values at various time scales; and P_i = predicted values. The nRMSE indicates modeling performance, with zero scores for nRMSE, rMBE, and RMSE representing perfect accuracy. A coefficient of determination score of 1 indicates a perfect fit, meaning predictions align exactly with the observed data. Achieving these optimal scores reflects the highest level of accuracy in predictive modeling (Veysi et al. 2023a).

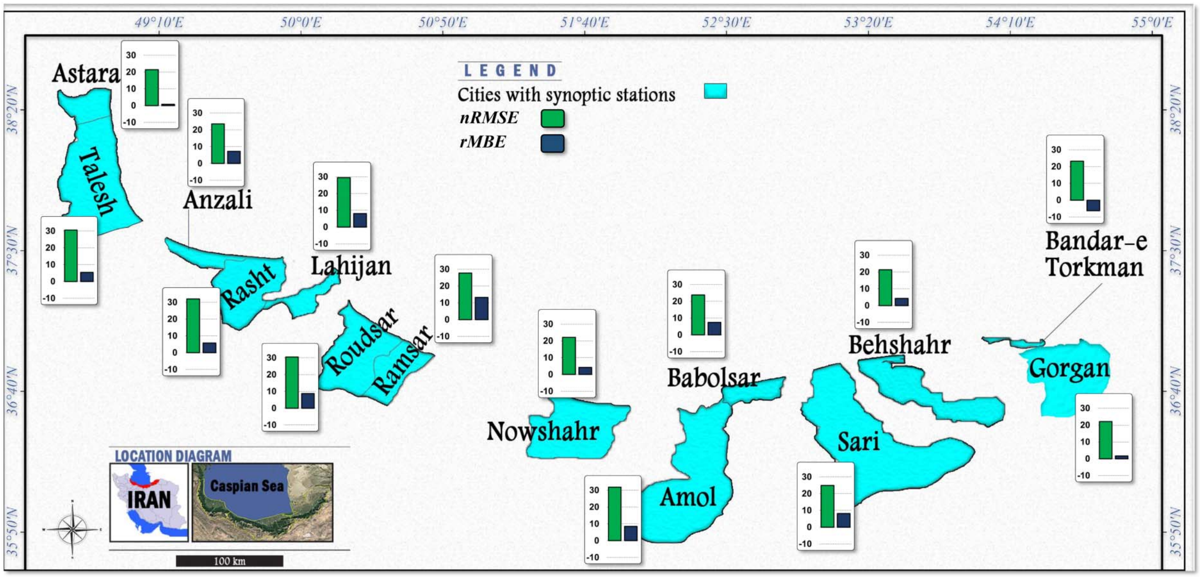

Fig. 9. nRMSE and rMBE values of ERA5 data set versus in suite ET_o. (Maps by author using ArcGIS © Esri.)

Results

Performance of ERA5 Reanalysis ET_o

This section highlights the main findings of the study, focusing on the use of ERA5 climate data as inputs for the FAO–Penman–Monteith equation to estimate daily ET_o. These results are compared with an alternative approach that employs ground-based observations of identical variables, gathered from 14 weather stations within the region. The statistical index values obtained from these stations are presented Fig. 9.

The high nRMSE values observed at specific stations can be attributed to a combination of geographical and climatic factors. In regions with uniform topography, such as coastal areas, ERA5 reanalysis data have demonstrated superior performance, indicating the data set's ability to provide relatively accurate ET_o estimates. However, in mountainous areas, the performance of ERA5 data weakens due to the complex interactions between topography and climate. Research by Raziei and Parehkar (2021) has shown that the application of ERA5 data in inappropriate topographic conditions, such as high-altitude regions, leads to higher bias values. Similarly, stations such as Astara, Ramsar, and Anzali, located near the northern slopes of the Alborz Mountain range, experience discrepancies due to their microclimatic variability and challenging terrain.

Coastal stations such as Nowshahr, situated near the Caspian Sea, are strongly influenced by the sea's moderating effects on temperature and humidity. Rapid and localized changes in these parameters, driven by sea breezes and fluctuating wind patterns, introduce variability that can challenge the accuracy of modeled ET_o.

Studies, such as Zhang et al. (2023), have emphasized the importance of bias correction methods for improving ET_o estimations. They demonstrated that raw and bias-corrected regional climate data exhibit differences in climatological spatial patterns and that applying bias correction methods effectively eliminates such discrepancies. This underscores the necessity of tailored correction methods, particularly in regions such as mountainous areas, where ERA5 data face limitations. To address these challenges, localized calibration of models and integration of high-resolution observational data are essential.

Bias Correction Estimated ET_o *with AI and ML Methods*

Given that the FAO–Penman–Monteith equation has gained global acceptance as a standard equation (Allen and Pruitt 1991), the ET_o derived from this equation with the input layer of weather station data are employed as target values. Fig. 10 elucidates the average of statistical analysis of different methods all over the coastline in both testing and training data sets.

Fig. 10 demonstrates that all methods achieve correlation coefficients exceeding 80% in both training and testing phases, indicating strong model performance. Due to the sensitivity of correlation coefficients to data volume, conclusions about time-series analyses are deferred. Instead, other statistical parameters were considered. Also, the RF and SVM methods illustrate similar and minimal average nRMSE and rMBE values. Notably, the GEP method exhibits inferior performance compared to other techniques due to its reliance on numerical models. This is aligned with the finding of Traore and Guven (2012), who also observed poor performance of GEP in modeling decadal ET_o in Burkina Faso. Citakoglu et al. (2014) reported reliable results for monthly mean ET_o in Turkey using ANN and ANFIS models, suggesting that these traditional methods perform well on larger temporal scales. However, on daily scales with large data sets, machine learning methods outperform. In a subsequent phase of the research, each station was individually examined as illustrated in Fig. 11.

Fig. 11 illustrates the results of five methods during training and testing. RF and SVM models outperformed other techniques for ET_o bias correction, aligning with previous research that demonstrates their effectiveness in estimating daily ET_o (Feng et al. 2017; Chen et al. 2020). The RF model met the criteria with rMBE values below 15% and nRMSE values under 10% for stations across various climates, except for Amol station, which showed nRMSE above 10%. Despite RF's general accuracy, there was overestimation indicated by positive rMBE values in both training and test stages.

Classic methods, such as GEP, performed poorly compared to ANN and ANFIS, showing significant bias. RF model accuracy decreased significantly in some stations, such as Talesh, whereas SVM showed more consistent results, suggesting superior generalizability across diverse data sets. Both RF and SVM showed overfitting, with the RF model more prone to this due to its higher R^2

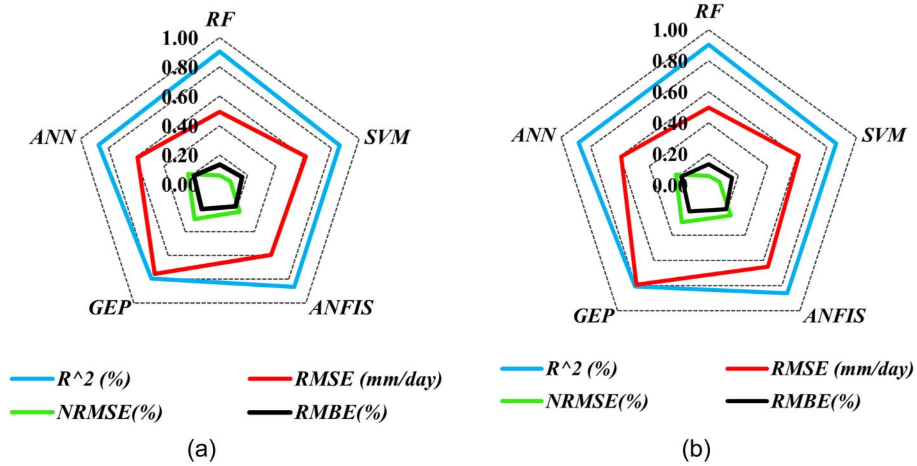

Fig. 10. Average of statistical analysis of different methods in all over of coastline: (a) train; and (b) test.

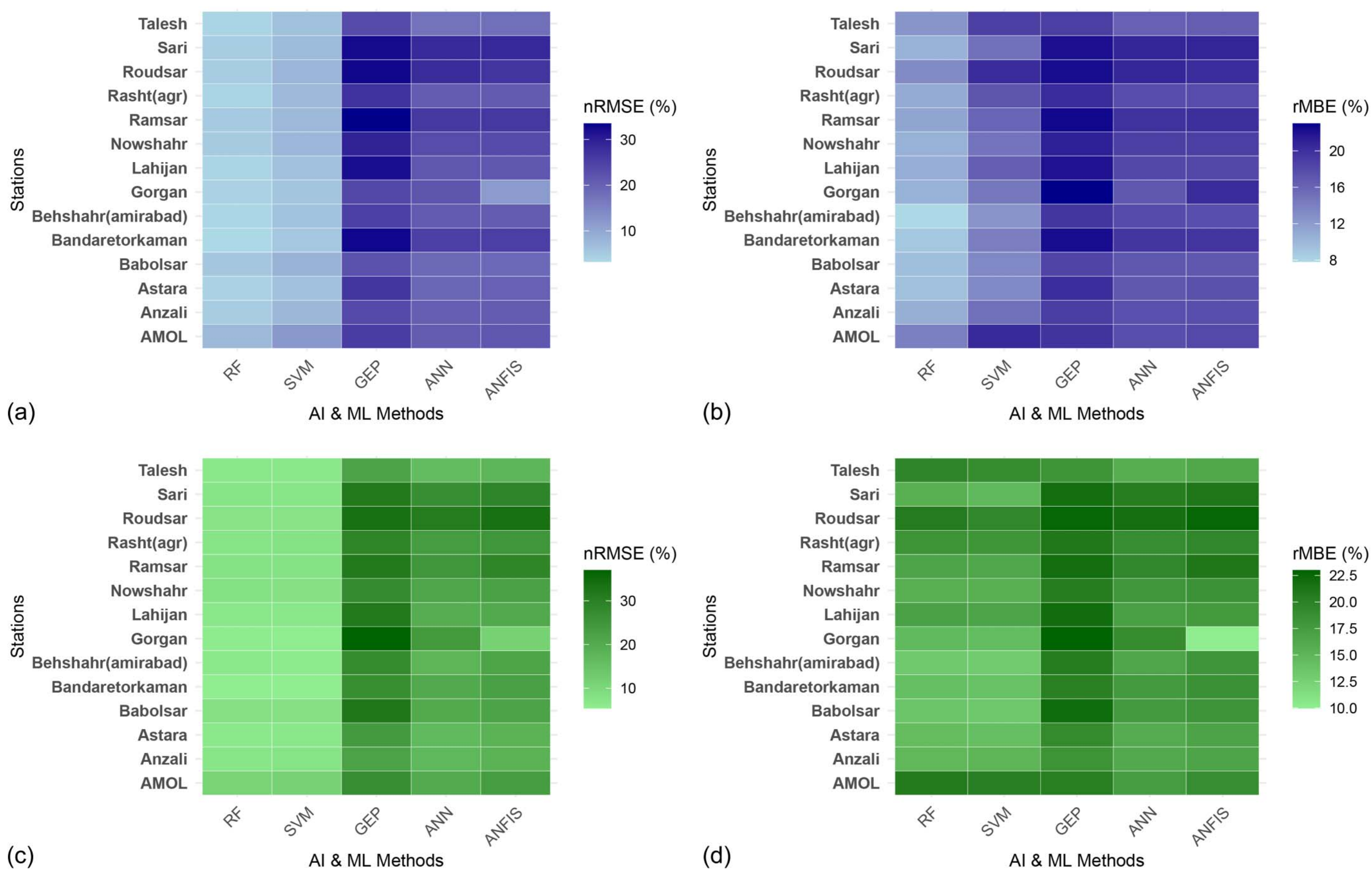

Fig. 11. nRMSE and rMBE of different methods across various stations: (a) heatmap of training nRMSE; and (b) rMBE, respectively. (c and d) Heatmap of testing nRMSE and rMBE, respectively.

and RMSE in training. The SVM model showed less overfitting, likely due to its built-in regularization. Introducing techniques such as early stopping could improve both models. The RF model achieved better average predictive accuracy for ET_o estimation, but the SVM model provided more stable predictions across geographically diverse stations. Future research could explore ensembles of SVM or hybrid models to leverage the strengths of both algorithms. All models showed greater accuracy in cold regions, with correlation values over 0.8. The highest RMSE was seen with GEP in hot, humid climates, while the lowest RMSE was with SVM and RF in cold climates. Both RF and SVM are more sensitive to outliers and noise compared to ANN, ANFIS, and GEP, which is crucial given the uncertainties and biases in reanalysis ET_o data. Overall, RF and SVM models aligned more closely with ET_o data from weather stations, especially along the Caspian Sea coastline.

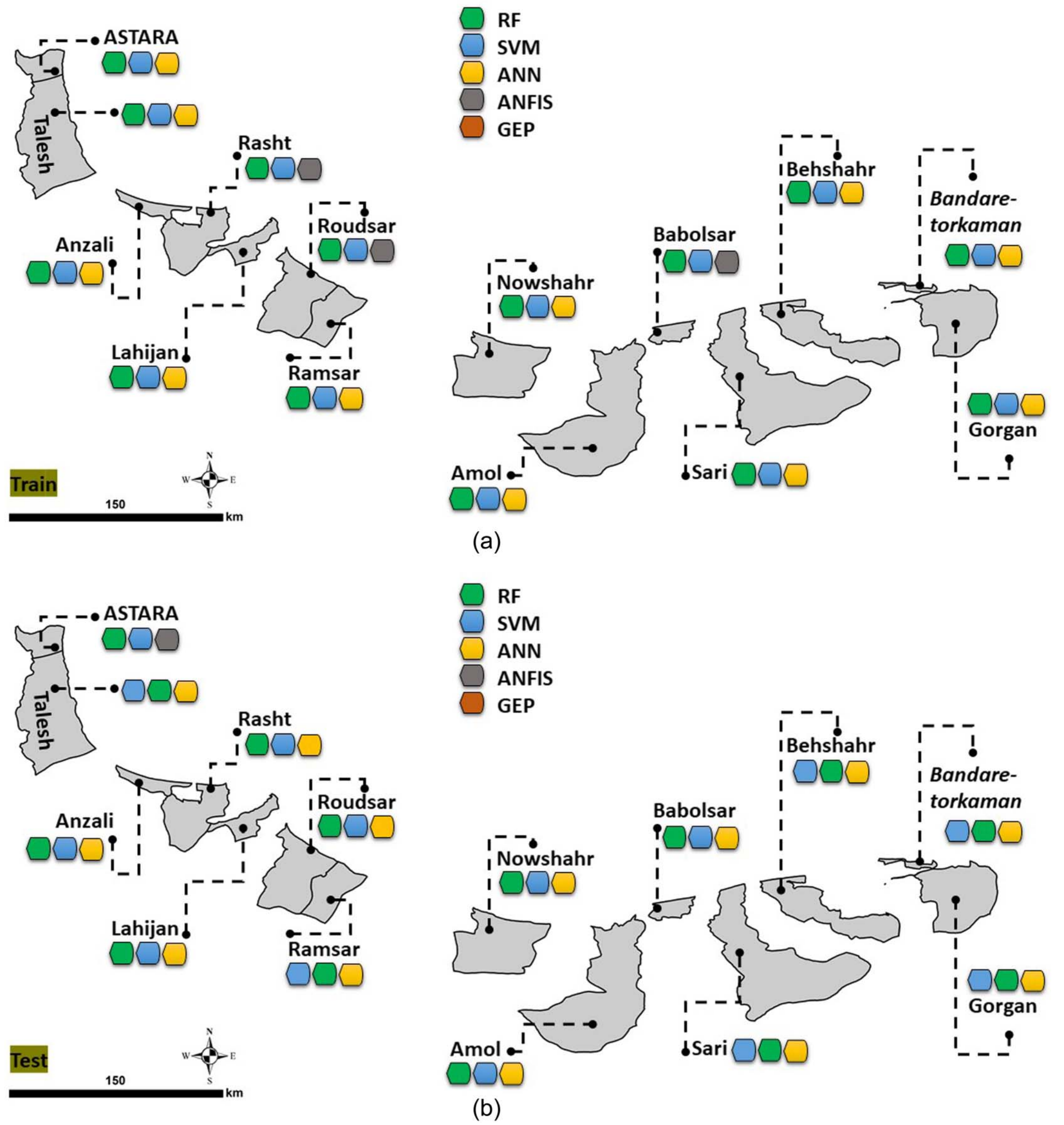

Fig. 12. Three top-performing data sets for bias correction of ERA5-derived daily ET_o along the Caspian Sea coastline: (a) performance for the training section; and (b) performance for the test section. The methods are distinguished by bar textures or shading patterns as follows: RF (light gray with diagonal lines), SVM (white with dots), ANN (medium gray), ANFIS (white with horizontal lines), and GEP (dark gray).

Map of Top-Performing AI Methods

As none of the ML methods achieved an nRMSE below 10% for ERA5 ET_o bias correction on their own, the top three performing methods were identified for each station based on their nRMSE ranking. Therefore, Fig. 12 illustrates that while RF generally excels during the training phase, SVM outperforms RF in certain stations during testing. This discrepancy may stem from SVM's ability to better handle variability in station specific climatic conditions, making it a more robust option for diverse geographical settings Fig. 12.

SVM outperforms in certain stations, such as Sari, Talesh, Gorgan, Ramsar, Behshahr, and Bandare-Torkaman. Mohammadrezapour et al. (2019) also found that SVM was superior to GEP and ANFIS for monthly ET_o forecasting. Kumar (2023) demonstrated that RF is effective for ET_o estimation with minimal climate data in semiarid regions. ANN ranks third, showing lower complexity and ease of use, while still outperforming GEP (Achite et al. 2022). Table 5 indicates that RF achieves the highest reduction in nRMSE for stations such as Rasht (87.71%) and Roudsar (84.25%) on training data, whereas SVM excels in some testing stations, outperforming RF. These findings suggest that SVM is particularly effective where RF underperforms. Table 5 illustrates while SVM is not consistently the top performer, it excels in some test data set stations, such as Bandare-Torkaman, Ramsar, Sari, Talesh, Behshahr, and Gorgan, outperforming RF. These results highlight SVM's potential in scenarios where RF is less effective.

Error Map for the Caspian Sea Basin

After determining that the RF method is the most suitable approach at the basin scale, we employed the co-kriging geostatistical interpolation method to interpolate error values across the entire basin, as depicted in Fig. 13.

The results of this interpolation reveal that hotspot error points are concentrated in the central region of the basin and around Mazandaran province, specifically in cities such as Amol, Noor, and Chalus. This information provides crucial insights for pinpointing

Table 5. Percent improvement in nRMSE of the top-performing method at each station

	Best model		nRMSE (%)			Enhance (%)	
Station	Train	Test	ERA5	Train	Test	Train	Test
AMOL	RF	RF	24.93	7.56	11.12	69.7	55.39
Anzali	RF	RF	23.57	4.87	7.17	79.32	69.56
Astara	RF	RF	21.38	4.04	6.58	81.13	69.25
Babolsar	RF	RF	23.82	5.62	8.37	76.4	64.86
B-torkaman	RF	SVM	23.26	3.26	5.41	86	76.75
Lahijan	RF	RF	29.45	3.79	6.90	87.11	76.58
Nowshahr	RF	RF	22.11	5.19	8.06	76.53	76.58
Ramsar	RF	SVM	27.76	5.11	7.75	81.6	72.09
Rasht	RF	RF	32.04	3.94	7.41	87.71	76.88
Roudsar	RF	RF	30.48	4.80	7.72	84.25	74.67
Sari	RF	SVM	24.95	4.76	7.08	80.92	71.62
Talesh	RF	SVM	30.60	3.71	6.82	87.9	77.71
Behshahr	RF	SVM	21.37	3.60	6.37	83.18	70.2
Gorgan	RF	SVM	22.08	4.03	5.66	81.74	74.36

areas where the establishment of additional synoptic stations may be beneficial in the future.

The analysis indicates that the reduction of reanalysis data errors can be effectively achieved through machine learning methods and geostatistical interpolation. This approach has the potential to initiate a new paradigm in related research. Our findings demonstrate that geostatistical methods better serve as essential tools for identifying error-prone areas. Ultimately, this can guide efforts to expand point-based stations in future developments.

Consequently, utilizing pixel-based data at large scales, obtained from reanalysis methods, in conjunction with machine learning techniques to minimize errors in this pixel-based data, is crucial. These types of data are not mutually exclusive; rather, they can complement each other effectively when applied correctly. By addressing error hotspots identified on the map, researchers can enhance data fidelity and improve model reliability, leading to more accurate environmental assessments and better-informed decision-making in agriculture water management studies.

General Discussion

Two common approaches to reduce bias in reanalysis-based ET_o estimation include correcting biases in the contributing meteorological factors and directly correcting the ET_o time series. The former method involves correcting biases in the individual meteorological variables used to calculate ET_o. The later approach focuses directly on correcting biases in the ET_o time series itself instead of adjusting individual meteorological variables (Nouri and Homaee 2022). In the first approach, it is crucial to correct all parameters for bias, as correcting only the most error-prone variable may inadvertently amplify the overall error. Since the ET_o equation involves interconnection of multiple variables, bias correction should be applied to all factors (Paredes et al. 2018). Bias correction of ET_o series is likely to be a more preferable alternative for ERA5; therefore in this research only the bias correction methods for ET_o values have been used.

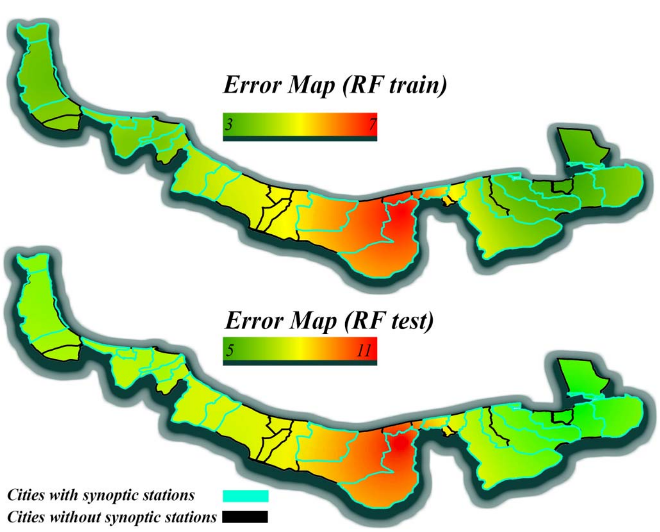

Fig. 13. Error maps for random forest training and testing.

Also, when we use AI/ML methods, the lengths of the training and testing data sets significantly influence the generalization, robustness, and accuracy of methods. In other words, large and representative data sets are essential for these models to learn the underlying patterns effectively and to perform well on unseen data. Limited training data may result in overfitting, causing the model to excel on the training set but perform poorly on new data, while inadequate testing data can impede a precise assessment of the model's effectiveness. Thus, the careful selection and appropriate sizing of training and testing data sets is crucial to ensure the reliability and applicability of AI/ML methods in estimating ET_o and other hydrological variables (Mohammadi and Mehdizadeh 2020). Kazemi et al. (2020) examined different ways to divide temporal data for estimating ET_o with machine learning in arid regions. Our current study, however, focuses only on the accuracy of various ET_o models, without considering their efficiency or complexity.

The results indicate that the RF machine learning model outperformed other methods in correcting biases in ET_o calculations fed with ERA5 data. RF demonstrates robustness in addressing nonlinear problems, contributing to its exceptional performance. Moreover, models trained on randomly sampled posttraining stations successfully passed validation tests, suggesting the spatial applicability of the RF method across various climate zones. This underscores its potential utility in correcting ET_o values even in regions with limited data availability.

In the northern regions of the Iran, it is accurate that the data show areas characterized by flatness and homogeneity. Nevertheless, a significant factor influencing error values, even during the validation stage, is the prevalence of widespread precipitation in these areas. Precipitation, which generally has an indirect impact on solar radiation levels, combined with the cloudy nature of the region, can lead to inaccuracies. A key factor for investigating bias is rainfall that has a nonlinear effect (Elagib et al. 2024). To put it differently, with ET_o in the coastal areas of Iran, errors may arise not only due to wind-related factors caused by the lack of vapor pressure deficit but also due to cloud cover affecting solar radiation. Essentially, these regions are constrained by energy limitations. Improvement of gridded meteorological model inputs, wind speed, and solar radiation may also lead to improved reanalysis performance.

While the RF method in this study have notably improved daily bias correction accuracy within ERA5 data, it is imperative to acknowledge certain limitations and expand on how current limitations can be overcome, such as using remote sensing data or low-cost technologies. Additionally, regarding ET_o interpolation accuracy, geostatistical methods, although widely used for their computational efficiency, fall short in accounting for topographical influences on ET_o dynamics (Barideh et al. 2022). Additionally, inherent errors in the ERA5 data set present challenges, especially in improving the accuracy of daily-scale estimates. Based on the study's findings, it is recommended to integrate RF and SVM models with real-time sensor data to improve bias correction in regions with limited ground-based weather stations. This hybrid approach could significantly enhance ET_o accuracy for irrigation scheduling in agricultural regions. Although bias correction methodologies strive to mitigate density dependencies, training data prerequisites persist. Nouri and Veysi (2024) found that combining several data sets provides more reliable results than hybridizing different machine learning methods. Therefore, another limitation to consider is the exclusive use of ERA5 data for bias correction. Combining data sets such as ERA5, NCEP, and GLEAM can outperform using a single method, such as RF-based bias correction. In other words, ensemble approaches with multiple data sets are more powerful than hybridizing different machine learning methods. Another limitation of this study is its focus on a single area along the Caspian Sea coastline. The predictive accuracy might be affected by wider and more irregular climatic fluctuations. Future research will address this by investigating these conditions and evaluating the introduced models' effectiveness for long-term forecasts.

Conclusion

This study has focused on bias correction of ERA5 ET_o across various environments, specifically in humid, subhumid, and dry subhumid areas situated along the coastline of the Caspian Sea basin north of Iran. The study investigated five methods include (i.e., ANN, ANFIS, GEP, RF, and SVM). Considering the broad scope of climatic zones covered in this study, one could argue that the findings are applicable to other case studies conducted in similar conditions.

In many studies, the ERA5 product is used in hydrological modeling. However, the approach taken in this model suffers from a limitation present in many studies: uncertainty associated with observations. Moreover, the quality of this spatial product is highly dependent on topographic conditions. Therefore, it is crucial to correct the daily ET_o estimates from ERA5 for any underestimation or overestimation in specific locations. In terms of bias correction between reanalysis ET_o and field data, ERA5 ET_o should undergo calibration before being applied in hydrological, agricultural, and erosion studies. RF and SVM models are preferred due to their robustness, flexibility, and interpretability, making them ideal for scenarios with limited data or complex climatic conditions. Among the methods assessed, RF outperformed others, making it the preferred model for detecting spatial patterns of ET_o, especially in areas without meteorological stations. When station data are unavailable, combining reanalysis data with appropriate AI methods is recommended for estimating ET_o. For instance, in coastal regions, using RF methods can significantly improve data accuracy. This approach aims to boost the confidence of water resource managers, farmers, scientists, and other users in the reanalysis data set. Future studies should explore the estimation of ET_o using other reanalysis products and machine learning techniques to enhance the accuracy of ET_o estimations over extended periods. Overall, this study provides a valuable framework for improving ET_o estimation in coastal regions with scarce meteorological data. The integration of machine learning techniques such as RF and SVM can aid in more accurate water management practices, particularly in areas with complex climatic conditions.

Data Availability Statement

Some or all data, models, or code that support the findings of this study are available from the corresponding author upon reasonable request.

Acknowledgments

The author would like to express their sincere gratitude to the Soil and Water Research Institute for its invaluable support and funding of this project. The institute's resources and expertise were instrumental in ensuring the successful completion of this work.

Author Contributions

Shadman Veysi: Conceptualization; Methodology; Supervision; Writing–original draft; Writing–review and editing. Soheila Zarei: Methodology; Writing–original draft; Writing–review and editing. Eslam Galehban: Data curation; Formal analysis; Investigation; Visualization. Amir Tahooni: Software; Validation; Visualization.

References

Achite, M., M. Jehanzaib, M. T. Sattari, A. K. Toubal, N. Elshaboury, A. Wałęga, N. Krakauer, J.-Y. Yoo, and T.-W. Kim. 2022. "Modern techniques to modeling reference evapotranspiration in a semiarid area based on ANN and GEP models." *Water* 14 (8): 1210. https://doi.org/10.3390/w14081210.

Ahmadaali, K., A. M. Liaghat, N. Heydari, and O. B. Haddad. 2013. "Application of artificial neural network and adaptive neural-based fuzzy inference system techniques in estimating of virtual water." *Int. J. Comput. Appl.* 76 (6): 12–19. https://doi.org/10.5120/13250-0715.

Allen, R. G., L. S. Pereira, D. Raes, and M. Smith. 1998. "Crop evapotranspiration-Guidelines for computing crop water requirements-FAO Irrigation and drainage paper 56." *FAO Rome* 300 (9): D05109.

Allen, R. G., and W. O. Pruitt. 1991. "FAO-24 reference evapotranspiration factors." *J. Irrig. Drain. Eng.* 117 (5): 758–773. https://doi.org/10.1061/(ASCE)0733-9437(1991)117:5(758).

Almorox, J., V. H. Quej, and P. Martí. 2015. "Global performance ranking of temperature-based approaches for evapotranspiration estimation considering Köppen climate classes." *J. Hydrol.* 528 (Sep): 514–522. https://doi.org/10.1016/j.jhydrol.2015.06.057.

Azadbakht, M., C. S. Fraser, and K. Khoshelham. 2018. "Synergy of sampling techniques and ensemble classifiers for classification of urban environments using full-waveform LiDAR data." *Int. J. Appl. Earth Obs. Geoinf.* 73 (Dec): 277–291. https://doi.org/10.1016/j.jag.2018.06.009.

Barideh, R., S. Veysi, N. Ebrahimipak, and N. Davatgar. 2022. "The challenge of reference evapotranspiration between the WaPOR data set and geostatistical methods." *Irrig. Drain.* 71 (5): 1268–1279. https://doi.org/10.1002/ird.2738.

Belgiu, M., and L. Drăguţ. 2016. "Random forest in remote sensing: A review of applications and future directions." *ISPRS J. Photogramm. Remote Sens.* 114 (Apr): 24–31. https://doi.org/10.1016/j.isprsjprs.2016.01.011.

Breiman, L. 2001. "Random forests." *Mach. Learn.* 45 (Oct): 5–32. https://doi.org/10.1023/A:1010933404324.

Chen, J., F. P. Brissette, D. Chaumont, and M. Braun. 2013. "Finding appropriate bias correction methods in downscaling precipitation for hydrologic impact studies over North America." *Water Resour. Res.* 49 (7): 4187–4205. https://doi.org/10.1002/wrcr.20331.

Chen, Z., Z. Zhu, H. Jiang, and S. Sun. 2020. "Estimating daily reference evapotranspiration based on limited meteorological data using deep learning and classical machine learning methods." *J. Hydrol.* 591 (Dec): 125286. https://doi.org/10.1016/j.jhydrol.2020.125286.

Citakoglu, H., M. Cobaner, T. Haktanir, and O. Kisi. 2014. "Estimation of monthly mean reference evapotranspiration in Turkey." *Water Resour. Manage.* 28 (Jan): 99–113. https://doi.org/10.1007/s11269-013-0474-1.

Deka, P. C. 2014. "Support vector machine applications in the field of hydrology: A review." *Appl. Soft Comput.* 19 (Jun): 372–386. https://doi.org/10.1016/j.asoc.2014.02.002.

Dimitriadou, S., and K. G. Nikolakopoulos. 2022. "Artificial neural networks for the prediction of the reference evapotranspiration of the Peloponnese Peninsula, Greece." *Water* 14 (13): 2027. https://doi.org/10.3390/w14132027.

Ebrahimy, H., H. Aghighi, M. Azadbakht, M. Amani, S. Mahdavi, and A. A. Matkan. 2021. "Downscaling MODIS land surface temperature product using an adaptive random forest regression method and Google Earth Engine for a 19-years spatiotemporal trend analysis over Iran." *IEEE J. Sel. Top. Appl. Earth Obs. Remote Sens.* 14 (Jan): 2103–2112. https://doi.org/10.1109/JSTARS.2021.3051422.

Elagib, N. A., M. M. Ali, and K. Schneider. 2024. "Evaluation and bias correction of CRU TS4.05 potential evapotranspiration across vast environments with limited data." *Atmos. Res.* 299 (Apr): 107194. https://doi.org/10.1016/j.atmosres.2023.107194.

Eslamian, S. S., S. A. Gohari, M. Biabanaki, and R. Malekian. 2008. "Estimation of monthly pan evaporation using artificial neural networks and support vector machines." *J. Appl. Sci.* 8 (19): 3497–3502. https://doi.org/10.3923/jas.2008.3497.3502.

Fan, J., W. Yue, L. Wu, F. Zhang, H. Cai, X. Wang, X. Lu, and Y. Xiang. 2018. "Evaluation of SVM, ELM and four tree-based ensemble models for predicting daily reference evapotranspiration using limited meteorological data in different climates of China." *Agric. For. Meteorol.* 263 (Dec): 225–241. https://doi.org/10.1016/j.agrformet.2018.08.019.

Farooque, A. A., H. Afzaal, F. Abbas, M. Bos, J. Maqsood, X. Wang, and N. Hussain. 2022. "Forecasting daily evapotranspiration using artificial neural networks for sustainable irrigation scheduling." *Irrig. Sci.* 2022 (Jan): 1–15. https://doi.org/10.1007/s00271-021-00751-1.

Feng, Y., N. Cui, D. Gong, Q. Zhang, and L. Zhao. 2017. "Evaluation of random forests and generalized regression neural networks for daily reference evapotranspiration modelling." *Agric. Water Manage.* 193 (Nov): 163–173. https://doi.org/10.1016/j.agwat.2017.08.003.

Ferreira, C. 2001. "Gene expression programming: A new adaptive algorithm for solving problems." Preprint, submitted December 30, 2001. https://arxiv.org/abs/cs/0102027.

Ferreira, C. 2006. "Designing neural networks using gene expression programming." In *Applied soft computing technologies: The challenge of complexity.* 517–535. Berlin: Springer.

Gebrechorkos, S. H., S. Hülsmann, and C. Bernhofer. 2018. "Evaluation of multiple climate data sources for managing environmental resources in East Africa." *Hydrol. Earth Syst. Sci.* 22 (8): 4547–4564. https://doi.org/10.5194/hess-22-4547-2018.

Gong, Y., Y. Zhang, S. Lan, and H. Wang. 2016. "A comparative study of artificial neural networks, support vector machines and adaptive neuro fuzzy inference system for forecasting groundwater levels near Lake Okeechobee, Florida." *Water Resour. Manage.* 30 (Jan): 375–391. https://doi.org/10.1007/s11269-015-1167-8.

Goyal, P., S. Kumar, and R. Sharda. 2023. "A review of the artificial intelligence (AI) based techniques for estimating reference evapotranspiration: Current trends and future perspectives." *Comput. Electron. Agric.* 209 (Jun): 107836. https://doi.org/10.1016/j.compag.2023.107836.

Granata, F., and F. Di Nunno. 2021. "Forecasting evapotranspiration in different climates using ensembles of recurrent neural networks." *Agric. Water Manage.* 255 (Sep): 107040. https://doi.org/10.1016/j.agwat.2021.107040.

Hersbach, H., et al. 2020. "The ERA5 global reanalysis." *Q. J. R. Meteorol. Soc.* 146 (730): 1999–2049. https://doi.org/10.1002/qj.3803.

Jang, J. S. 1993. "ANFIS: Adaptive-network-based fuzzy inference system." *IEEE Trans. Syst. Man Cybern.* 23 (3): 665–685. https://doi.org/10.1109/21.256541.

Ji, X., Y. Li, X. Luo, D. He, R. Guo, J. Wang, Y. Bai, C. Yue, and C. Liu. 2020. "Evaluation of bias correction methods for APHRODITE data to improve hydrologic simulation in a large Himalayan basin." *Atmos. Res.* 242 (Sep): 104964. https://doi.org/10.1016/j.atmosres.2020.104964.

Karaboga, D., and E. Kaya. 2019. "Adaptive network based fuzzy inference system (ANFIS) training approaches: A comprehensive survey." *Artif. Intell. Rev.* 52 (Dec): 2263–2293. https://doi.org/10.1007/s10462-017-9610-2.

Kazemi, M. H., J. Shiri, P. Marti, and A. Majnooni-Heris. 2020. "Assessing temporal data partitioning scenarios for estimating reference evapotranspiration with machine learning techniques in arid regions." *J. Hydrol.* 590 (Nov): 125252. https://doi.org/10.1016/j.jhydrol.2020.125252.

Keshtegar, B., O. Kisi, H. Ghohani Arab, and M. Zounemat-Kermani. 2018. "Subset modeling basis ANFIS for prediction of the reference evapotranspiration." *Water Resour. Manage.* 32 (Feb): 1101–1116. https://doi.org/10.1007/s11269-017-1857-5.

Khan, M. S., and P. Coulibaly. 2006. "Application of support vector machine in lake water level prediction." *J. Hydrol. Eng.* 11 (3): 199–205. https://doi.org/10.1061/(ASCE)1084-0699(2006)11:3(199).

Kisi, O., and M. Zounemat-Kermani. 2014. "Comparison of two different adaptive neuro-fuzzy inference systems in modelling daily reference evapotranspiration." *Water Resour. Manage.* 28 (Jul): 2655–2675. https://doi.org/10.1007/s11269-014-0632-0.

Kumar, U. 2023. "Modelling monthly reference evapotranspiration estimation using machine learning approach in data-scarce North Western Himalaya region (Almora), Uttarakhand." *J. Earth Syst. Sci.* 132 (3): 129. https://doi.org/10.1007/s12040-023-02138-6.

Landeras, G., A. Ortiz-Barredo, and J. J. López. 2008. "Comparison of artificial neural network models and empirical and semi-empirical equations for daily reference evapotranspiration estimation in the Basque Country (Northern Spain)." *Agric. Water Manage.* 95 (5): 553–565. https://doi.org/10.1016/j.agwat.2007.12.011.

Liaw, A. 2002. "Classification and regression by randomForest." *R News* 2 (3): 18–22.

López-Urrea, R., F. M. de Santa Olalla, C. Fabeiro, and A. Moratalla. 2006. "Testing evapotranspiration equations using lysimeter observations in a semiarid climate." *Agric. Water Manage.* 85 (1–2): 15–26. https://doi.org/10.1016/j.agwat.2006.03.014.

Mandal, N., and K. Chanda. 2023. "Performance of machine learning algorithms for multi-step ahead prediction of reference evapotranspiration across various agro-climatic zones and cropping seasons." *J. Hydrol.* 620 (May): 129418. https://doi.org/10.1016/j.jhydrol.2023.129418.

Martins, D. S., P. Paredes, T. Raziei, C. Pires, J. Cadima, and L. S. Pereira. 2017. "Assessing reference evapotranspiration estimation from reanalysis weather products." *Int. J. Climatol.* 37 (5): 2378–2397. https://doi.org/10.1002/joc.4852.

Mehdizadeh, S., and A. Kozekalani Sales. 2018. "A comparative study of autoregressive, autoregressive moving average, gene expression programming and Bayesian networks for estimating monthly streamflow." *Water Resour. Manage.* 32 (Jul): 3001–3022. https://doi.org/10.1007/s11269-018-1970-0.

Mehr, A. D. 2018. "An improved gene expression programming model for streamflow forecasting in intermittent streams." *J. Hydrol.* 563 (Aug): 669–678. https://doi.org/10.1016/j.jhydrol.2018.06.049.

Mohammadi, B., and S. Mehdizadeh. 2020. "Modeling daily reference evapotranspiration via a novel approach based on support vector regression coupled with whale optimization algorithm." *Agric. Water Manage.* 237 (Jul): 106145. https://doi.org/10.1016/j.agwat.2020.106145.

Mohammadrezapour, O., J. Piri, and O. Kisi. 2019. "Comparison of SVM, ANFIS and GEP in modeling monthly potential evapotranspiration in an arid region (Case study: Sistan and Baluchestan Province, Iran)." *Water Supply* 19 (2): 392–403. https://doi.org/10.2166/ws.2018.084.

Moyers, K., R. Sabie, E. Waring, J. Preciado, C. C. Naughton, T. Harmon, and J. H. Viers. 2023. "A decade of data-driven water budgets: Synthesis and bibliometric review." *Water Resour. Res.* 59 (11): e2022WR034310. https://doi.org/10.1029/2022WR034310.

Nasrabadi, T., G. Nabi Bidhendi, A. Karbassi, P. Grathwohl, and N. Mehrdadi. 2011. "Impact of major organophosphate pesticides used in agriculture to surface water and sediment quality (Southern Caspian Sea basin, Haraz River)." *Environ. Earth Sci.* 63 (Jun): 873–883. https://doi.org/10.1007/s12665-010-0757-2.

Nourani, V., G. Elkiran, and J. Abdullahi. 2020. "Multi-step ahead modeling of reference evapotranspiration using a multi-model approach." *J. Hydrol.* 581 (Feb): 124434. https://doi.org/10.1016/j.jhydrol.2019.124434.

Nouri, M., and M. Homaee. 2022. "Reference crop evapotranspiration for data-sparse regions using reanalysis products." *Agric. Water Manage.* 262 (Mar): 107319. https://doi.org/10.1016/j.agwat.2021.107319.

Nouri, M., and S. Veysi. 2024. "CMIP6 multi-model ensemble projection of reference evapotranspiration using machine learning algorithms." *Agric. Water Manage.* 306 (Dec): 109190. https://doi.org/10.1016/j.agwat.2024.109190.

Paredes, P., D. S. Martins, J. Cadima, C. Pires, and L. S. Pereira. 2017. "Accuracy of daily PM-ETo estimations with ERA-Interim reanalysis products." *Eur. Water* 59 (32): 239–246.

Paredes, P., D. S. Martins, L. S. Pereira, J. Cadima, and C. Pires. 2018. "Accuracy of daily estimation of grass reference evapotranspiration using ERA-Interim reanalysis products with assessment of alternative bias correction schemes." *Agric. Water Manage.* 210 (Nov): 340–353. https://doi.org/10.1016/j.agwat.2018.08.003.

Peel, M. C., B. L. Finlayson, and T. A. McMahon. 2007. "Updated world map of the Köppen-Geiger climate classification." *Hydrol. Earth Syst. Sci.* 11 (5): 1633–1644. https://doi.org/10.5194/hess-11-1633-2007.

Pelosi, A. 2023. "Performance of the Copernicus European Regional Reanalysis (CERRA) dataset as proxy of ground-based agrometeorological data." *Agric. Water Manage.* 289 (Nov): 108556. https://doi.org/10.1016/j.agwat.2023.108556.

Pereira, L. S., R. G. Allen, M. Smith, and D. Raes. 2015. "Crop evapotranspiration estimation with FAO56: Past and future." *Agric. Water Manage.* 147 (Jan): 4–20. https://doi.org/10.1016/j.agwat.2014.07.031.

Pereira, L. S., P. Paredes, D. J. López-Urrea, and N. Jovanovic. 2021. "Updates and advances to the FAO56 crop water requirements method." *Agric. Water Manage.* 248 (Apr): 106697. https://doi.org/10.1016/j.agwat.2020.106697.

Rahimikhoob, H., T. Sohrabi, and M. Delshad. 2020. "Assessment of reference evapotranspiration estimation methods in controlled greenhouse conditions." *Irrig. Sci.* 38 (Jul): 389–400. https://doi.org/10.1007/s00271-020-00680-5.

Raziei, T., and A. Parehkar. 2021. "Performance evaluation of NCEP/NCAR reanalysis blended with observation-based datasets for estimating reference evapotranspiration across Iran." *Theor. Appl. Climatol.* 144 (May): 885–903. https://doi.org/10.1007/s00704-021-03578-0.

Rubel, F., K. Brugger, K. Haslinger, and I. Auer. 2017. "The climate of the European Alps: Shift of very high resolution Köppen-Geiger climate zones 1800–2100." *Meteorol. Z.* 26 (2): 115–125. https://doi.org/10.1127/metz/2016/0816.

Sentelhas, P. C., T. J. Gillespie, and E. A. Santos. 2010. "Evaluation of FAO Penman–Monteith and alternative methods for estimating reference evapotranspiration with missing data in Southern Ontario, Canada." *Agric. Water Manage.* 97 (5): 635–644. https://doi.org/10.1016/j.agwat.2009.12.001.

Sharma, G., A. Singh, and S. Jain. 2022. "A hybrid deep neural network approach to estimate reference evapotranspiration using limited climate data." In *Neural computing and applications*, 1–20. Berlin: Springer. https://doi.org/10.1007/s00521-021-06661-9.

Shiri, J. 2017. "Evaluation of FAO56-PM, empirical, semi-empirical and gene expression programming approaches for estimating daily reference evapotranspiration in hyper-arid regions of Iran." *Agric. Water Manage.* 188 (Jul): 101–114. https://doi.org/10.1016/j.agwat.2017.04.009.

Shiri, J. 2019. "Modeling reference evapotranspiration in island environments: Assessing the practical implications." *J. Hydrol.* 570 (Mar): 265–280. https://doi.org/10.1016/j.jhydrol.2018.12.068.

Srivastava, P. K., T. Islam, M. Gupta, G. Petropoulos, and Q. Dai. 2015. "WRF dynamical downscaling and bias correction schemes for NCEP estimated hydro-meteorological variables." *Water Resour. Manage.* 29 (May): 2267–2284. https://doi.org/10.1007/s11269-015-0940-z.

Takagi, T., and M. Sugeno. 1985. "Fuzzy identification of systems and its applications to modeling and control." *IEEE Trans. Syst. Man Cyber.* 1 (Jan): 116–132. https://doi.org/10.1109/TSMC.1985.6313399.

Tao, H., Q. Li, Q. Zhou, J. Chen, B. Fu, J. Wang, W. Qin, J. Hou, J. Chen, L. Dong, and (on behalf of the CLIATHVR multicenter clinical study team). 2018. "A prediction study of warfarin individual stable dose after mechanical heart valve replacement: Adaptive neural-fuzzy inference system prediction." *BMC Surg.* 18 (Dec): 1–10. https://doi.org/10.1186/s12893-018-0343-1.

Traore, S., and A. Guven. 2012. "Regional-specific numerical models of evapotranspiration using gene-expression programming interface in Sahel." *Water Resour. Manage.* 26 (Dec): 4367–4380. https://doi.org/10.1007/s11269-012-0149-3.

Traore, S., Y. Luo, and G. Fipps. 2016. "Deployment of artificial neural network for short-term forecasting of evapotranspiration using public weather forecast restricted messages." *Agric. Water Manage.* 163 (Jan): 363–379. https://doi.org/10.1016/j.agwat.2015.10.009.

Veysi, S., and E. Galehban. 2024. "Chapter 4—Conceptual of soil moisture based on remote sensing and reanalysis dataset." In *Remote sensing of soil and land surface processes monitoring, mapping, and modeling*, edited by A. M. Melesse, O. Rahmati, K. Khosravi, and G. P. Petropoulos, 77–98. Amsterdam, Netherlands: Elsevier.

Veysi, S., A. Heidari Motlagh, A. H. Nasrolahi, and A. R. Safi. 2023a. "A new approach to estimate daily evapotranspiration, based on Landsat data and FAO56 principles." *Int. J. Remote Sens.* 44 (15): 4727–4752. https://doi.org/10.1080/01431161.2023.2237662.

Veysi, S., M. Nouri, and A. Jabbari. 2023b. "Performance evaluation of WaPOR and ERA5 datasets for the purpose of estimating reference evapotranspiration in the caspian sea basin." *J. Water Res. Agric.* 37 (2): 193–206. https://doi.org/10.22092/jwra.2023.361653.981.

Veysi, S., M. Nouri, and A. Jabbari. 2024. "Reference evapotranspiration estimation using reanalysis and WaPOR products in dryland Croplands." *Heliyon* 10 (4): e26531. https://doi.org/10.1016/j.heliyon.2024.e26531.

Wen, X., J. Si, Z. He, J. Wu, H. Shao, and H. Yu. 2015. "Support-vector-machine-based models for modeling daily reference evapotranspiration with limited climatic data in extreme arid regions." *Water Resour. Manage.* 29 (Jul): 3195–3209. https://doi.org/10.1007/s11269-015-0990-2.

Yassin, M. A., A. A. Alazba, and M. A. Mattar. 2016. "Artificial neural networks versus gene expression programming for estimating reference evapotranspiration in arid climate." *Agric. Water Manage.* 163 (Jan): 110–124. https://doi.org/10.1016/j.agwat.2015.09.009.

Yin, Z., X. Wen, Q. Feng, Z. He, S. Zou, and L. Yang. 2017. "Integrating genetic algorithm and support vector machine for modeling daily reference evapotranspiration in a semi-arid mountain area." *Hydrol. Res.* 48 (5): 1177–1191. https://doi.org/10.2166/nh.2016.205.

Zakeri, R., and P. Shankar. 2022. "A neural network-augmented Bayesian approach to uncertain parameter estimation in nonlinear dynamic systems." In *Proc., ASME Int. Mechanical Engineering Congress and Exposition*. New York: American Society of Mechanical Engineers.

ZamanZad-Ghavidel, S., O. Bozorg-Haddad, and E. Goharian. 2021. "Sustainability assessment of water resource systems using a novel hydro-socio-economic index (HSEI)." *Environ. Dev. Sustainability* 23 (Feb): 1869–1916. https://doi.org/10.1007/s10668-020-00655-8.

Zhang, H., S. Chapman, R. Trancoso, N. Toombs, and J. Syktus. 2023. "The impact of bias correction on reference evapotranspiration and its climate change signal." In *Proc., 25th Int. Congress on Modelling and Simulation*, 1102–1108. Canberra, ACT, Australia: Modelling and Simulation Society of Australia and New Zealand.

Zhao, Y., J. Zhang, Y. Bai, S. Zhang, S. Yang, M. Henchiri, A. M. Seka, and L. Nanzad. 2022. "Drought monitoring and performance evaluation based on machine learning fusion of multi-source remote sensing drought factors." *Remote Sens.* 14 (24): 6398. https://doi.org/10.3390/rs14246398.

J. Irrig. Drain Eng., 2025, 151(4): 04025021